

Efficient Federated Split Learning for Large Language Models over Communication Networks

Kai Zhao, Zhaohui Yang

Abstract—Fine-tuning pre-trained large language models (LLM) in a distributed manner poses significant challenges on resource-constrained edge devices. To address this challenge, we propose FedsLLM, a novel framework that integrates split federated learning with parameter-efficient fine-tuning techniques. By leveraging model splitting and Low-Rank Adaptation (LoRA), FedsLLM reduces the computational burden on edge devices. Furthermore, the introduction of a federated server facilitates parallel training and enhances privacy. To accommodate heterogeneous communication conditions and diverse computational capabilities of edge devices, as well as the impact of LoRA rank selection on model convergence and training cost, we formulate a joint optimization problem. The formulated problem jointly optimizes subchannel allocation, power control, model splitting point selection, and LoRA rank configuration, all aimed at minimizing total training delay. An alternating optimization algorithm is developed to efficiently solve this problem and accelerate the training process. Simulation results demonstrate that the proposed FedsLLM framework achieves comparable model accuracy while significantly reducing client-side computational requirements. Furthermore, the proposed resource allocation scheme and adaptive LoRA rank selection strategy notably reduce the training latency compared to conventional approaches.

Index Terms—Split federated learning, large language models, resource management, low-rank adaptation, edge intelligence.

I. INTRODUCTION

THE rapid advancement of pre-trained models has significantly advanced fields such as computer vision and natural language processing [3], [4]. According to scaling laws [5], increasing the number of model parameters and training data volume typically leads to improved model performance. Meanwhile, with the proliferation of Internet of Things (IoT) devices and sensors within wireless networks, edge devices have become capable of generating and collecting vast amounts of data. Effectively leveraging this distributed data can further enhance model performance. However, due to privacy concerns and communication constraints [6], [7], transmitting raw data to a central server is often impractical. To overcome these challenges, Federated Learning (FL) has emerged as a promising paradigm for the distributed fine-tuning of large language models (LLM) [8]–[10]. FL preserves privacy and reduces communication overhead by transmitting model parameters rather than raw data [11].

Nevertheless, as the size of models continues to increase, fully loading and fine-tuning these large-scale models on resource-limited edge devices remains computationally infeasible. To mitigate this challenge, Split Learning (SL) has been proposed [12], which partitions the model and offloads computationally intensive tasks to a more resourceful server. Instead of exchanging entire model parameters, SL allows clients

to transmit only intermediate activations and corresponding gradients, thereby substantially reducing communication overhead [13], [14]. However, a critical drawback of SL is its dependence on sequential interactions between clients and the server, severely restricting the overall training efficiency. To address this limitation, Split Federated Learning (SFL) has been recently introduced, effectively combining the privacy preservation and parallelization advantages of FL with the communication efficiency of SL [15]. Consequently, SFL is emerging as a highly promising framework for distributed training across heterogeneous edge computing environments.

Fine-tuning pre-trained models on downstream tasks typically yields substantial improvements in performance. However, as the scale of model parameters increases, performing full fine-tuning becomes computationally prohibitive due to intensive resource requirements. While model quantization provides a promising approach for reducing computational overhead by compressing models, it typically requires specialized hardware capable of low-bit computations. A more practical and hardware-compatible approach is Low-Rank Adaptation (LoRA) [16], [17], which introduces trainable low-rank modules into the existing model structure, significantly decreasing the number of trainable parameters while maintaining comparable performance to full fine-tuning. When combined with SFL, LoRA further reduces client-side computational workload and the volume of uploaded data, enabling more communication-efficient fine-tuning of large-scale models. Although prior studies have explored the integration of FL with LoRA, the combination of LoRA specifically with SFL remains under-explored in existing literature [21].

Although resource-rich cloud environments can easily accommodate the computational demands associated with large-scale models, resource-constrained edge devices typically lack such computational capacities. Therefore, minimizing computational overhead becomes essential for effective deployment in these edge computing scenarios. Furthermore, the straggler effect prevalent in SFL can significantly hinder training progress, thus efficient resource allocation strategies are vital for reducing latency and maintaining training efficiency. Additionally, existing studies often focus solely on a single training round and neglecting the comprehensive impact of model training hyperparameters on the total latency across the entire training process. Moreover, SFL involves extensive parameter exchanges between clients and two separate servers, where computation and communication are inherently coupled. Thus, jointly optimizing computation and communication processes represents a necessary and promising perspective for enhancing the efficiency of the training process [2].

In this paper, we propose FedsLLM, a novel split feder-

ated learning framework specifically designed for efficiently fine-tuning LLM within resource-constrained edge networks. FedsLLM integrates LoRA and SFL techniques to achieve efficient distributed training. The proposed framework leverages distributed co-training mechanisms to securely and effectively harness data dispersed across edge devices, while the use of model splitting significantly alleviates local resource requirements. Moreover, the incorporation of efficient fine-tuning techniques reduces both computational burden and communication overhead.

Nevertheless, due to the inherent heterogeneity in channel conditions and computational capabilities among edge devices, the emergence of stragglers can substantially degrade overall training efficiency [22], [23]. A appropriately designed resource allocation and model splitting strategy can mitigate the adverse impacts of stragglers and accelerate training speed, thereby enhancing overall learning efficiency. Additionally, the rank chosen for the LoRA module influences both computation complexity and communication overhead, thereby affecting the convergence speed of the training process. Proper selection of LoRA rank strikes a balance between these overheads and can significantly reduce total training delay.

To address these challenges, we formulate a comprehensive optimization problem for FedsLLM that involves subchannel assignment, power control, split layer selection, and rank selection. Subsequently, we develop an efficient algorithm to solve the formulated optimization problem. The primary contributions of this paper are summarized as follows:

- We introduce the FedsLLM framework, which effectively integrates SFL with LoRA techniques to facilitate efficient and distributed fine-tuning of LLM in edge computing environments.
- We comprehensively analyze how the selection of LoRA rank impacts both computational and communication costs as well as convergence speed, and accordingly propose an effective rank selection scheme to enhance training efficiency.
- We design an efficient resource allocation and task offloading strategy to jointly optimize subchannel assignment, power control, split location, and LoRA rank selection, aiming at minimizing the total training latency.
- We conduct extensive simulations to validate that the proposed FedsLLM framework efficiently accomplishes the fine-tuning task. Additionally, simulation results demonstrate that the proposed resource allocation and rank selection strategies significantly reduce training latency compared to traditional methods.

The remainder of this paper is organized as follows: Section II reviews related work. Sections III and IV introduce the system model and framework of FedsLLM, respectively. Sections V and VI detail the formulation of the resource management problem and the corresponding solution algorithm. Simulation results and analysis are provided in Section VII. Finally, conclusions are drawn in Section VIII.

II. RELATED WORK

FL is a widely used distributed learning framework that ensures privacy preservation while maintaining communication

efficiency. However, deploying FL effectively in edge network scenarios, where client devices have limited computational and communication resources, remains a critical challenge for improving performance [24]. A significant body of research has addressed this issue, focusing on model compression [28], resource allocation [26], hierarchical aggregation [27], and client selection [25]. SL mitigates some of these challenges by offloading the majority of the training workload to the server [14], reducing both computational cost and communication overhead on the client side. This capability, which addresses some of the limitations of FL [11], is gradually emerging as a promising distributed learning framework. However, in the early version of SL [12], the client could only perform training sequentially, severely limiting training efficiency. To overcome this, Split Federated Learning (SFL) [15], which combines the advantages of SL and FL, has been proposed. Given its notable benefits, extensive research has been conducted in areas such as model splitting [29], model aggregation [30], and client selection [31].

The effectiveness of SFL in small-scale models has been demonstrated in several studies. For example, a hierarchical SFL framework was proposed in [32] to address challenges such as single points of failure, fairness issues, and poor convergence rates, yielding good performance on the MNIST dataset. For client heterogeneity, a ring-topology-based SFL was proposed in [33], which demonstrated better convergence performance than benchmark methods on both the independent and identically distributed (IID) and non-IID datasets. This method was applied to mainstream networks such as ResNet18 [34], VGG16 [35], and AlexNet [36], while also preventing eavesdroppers from recovering training data. However, SFL for LLM remains an area that has not been fully explored. Some research has begun to focus on fine-tuning LLM using FL architectures for distributed collaborative training over wireless networks. For instance, [8] explores this approach, while [37] introduces low-parameter federated learning for cost-effective parameter construction, local model fine-tuning, and global model aggregation using soft labeling and LoRA. Additionally, [38] employs lightweight adapters in LLM to facilitate knowledge exchange between servers and clients, maintaining data privacy while minimizing overheads. While these studies emphasize lightweight techniques for efficient training and reduced client load, they fail to adequately address resource constraints on clients through model splitting deployment. In this paper, we provide an efficient resource-constrained fine-tuning approach for LLM by combining SFL with LoRA.

SFL involves extensive parameter exchanges over wireless networks, making it both an interesting and challenging problem to effectively utilize the resources available on edge devices and central servers. In [39], the authors consider a real-world scenario with heterogeneous devices and a single split point in a deep neural network. They formulate and solve a joint problem of split-point selection and bandwidth allocation to minimize system latency. [40] proposes an efficient parallel split learning algorithm that optimizes user-side workloads and server-side resource allocation while accounting for user heterogeneity. [32] introduces the hierarchical SFL framework,

TABLE I
SUMMARY OF KEY NOTATIONS

Notation	Description
K, \mathcal{K}	Number and set of participating clients.
\mathcal{D}_k, D_k	Local dataset of client k and its size.
D	Total samples, $D = \sum_{k=1}^K D_k$.
$E(r)$	Global rounds to reach target accuracy (depends on LoRA rank r).
I	Local client-server iterations per global round.
b	Mini-batch size.
ℓ_c, ℓ_s	Number of layers deployed on client/server, respectively.
$\mathbf{W}_c, \mathbf{W}_s$	Frozen pre-trained weights on client/server.
$\Delta \mathbf{W}_c, \Delta \mathbf{W}_s$	LoRA trainable weights on client/server.
r	LoRA rank (dimension of low-rank factors).
μ_j	Split flag: 1 if layer j on client, else 0.
f_k, f_s	Computing capability (cycles/s) of client k and main server.
κ_k, κ_s	GPU cycles required per FLOP on client/server.
$\rho_j, \Delta \rho_j$	FP FLOPs of base/LoRA module at layer j .
$\varpi_j, \Delta \varpi_j$	BP FLOPs of base/LoRA module at layer j .
ψ_j	Activation size (bits) at layer j .
$\Phi_c^{F/B}, \Delta \Phi_c^{F/B}$	Client-side FP/BP workload per sample.
$\Phi_s^{F/B}, \Delta \Phi_s^{F/B}$	Server-side FP/BP workload per sample.
Γ_s	Activation size per sample uploaded to main server.
$\Delta \Theta_c$	Size of client-side LoRA parameters (bits).
M, N	Number of sub-channels to main/federated server.
$r_k^{i,s}, r_k^{i,f}$	Binary sub-channel assignment indicators.
B_i^s, B_i^f	Bandwidth of sub-channel i .
p_i^s, p_i^f	Transmit PSD on sub-channel i .
G_c, G_s, G_f	Antenna gains of client, main server, federated server.
$\gamma(d_k^{s/f})$	Large-scale channel gain (client k to main/federated server).
$(\sigma^{s/f})^2$	Noise PSD on main/federated uplink.
R_k^s, R_k^f	Uplink rate of client k to main/federated server.
$p_k^{\max}, p_{th}^{\max}$	Per-client and network-wide power limits.
$\theta_{k,\xi}^s, \theta_{k,\xi}^f$	Auxiliary rate variables after log-convexification.
$T_k^F, T_k^s, T_k^B, T_k^f$	Client FP, activation-upload, BP, model-upload latency.
T_s^F, T_s^B	Server-side forward/backward latencies.
T_1, T_2, T_3	Worst-case delays: $\max_k (T_k^F + T_k^s), \max_k T_k^B, \max_k T_k^f$.
T_{local}, T	Single local-round latency and total training latency.

a) *Client-side Forward Propagation*: In this step, each participating client k randomly selects a mini-batch $\mathcal{B}_k \subseteq \mathcal{D}_k$ from its local dataset as input, where \mathcal{B}_k contains B_k data samples. Each client independently performs forward propagation (FP) on its respective segment of the model. Upon completion of client-side FP, activation vectors are generated at the split layer (the final layer of the client-side model). The activation vector output by the k -th client at the t -th training step can be expressed as:

$$\mathbf{s}_k^t = \varphi(\mathbf{W}_c | \Delta \mathbf{W}_c, k^{t-1}, \mathbf{x}_k^t), \quad (3)$$

where $\varphi(\mathbf{W} | \Delta \mathbf{W}, \mathbf{x})$ denotes the mapping between input data \mathbf{x} and the predicted output of the model, given pre-trained parameters \mathbf{W} and LoRA trainable parameters $\Delta \mathbf{W}$.

b) *Uploading of Activation Vectors*: After client-side forward propagation is completed, all participating clients transmit their activation vectors \mathbf{s}_k^t and the corresponding labels y_k^t to the main server over the wireless channel. Subsequently, the main server utilizes these collected activation vectors to perform further fine-tuning on the server-side model.

c) *Server-side Forward Propagation*: Upon receiving the activation vectors from clients, the main server inputs these vectors into the server-side model to perform forward propagation. Let $\Delta \mathbf{W}_s^{t-1}$ denote the LoRA trainable parameters of the server-side model at the $(t-1)$ -th training step. Thus, the predicted output of the main server for the t -th step can be expressed as:

$$\hat{y}_k^t = \varphi(\mathbf{W}_s | \Delta \mathbf{W}_s^{t-1}, \mathbf{S}^t), \quad (4)$$

where $\mathbf{S}^t = [\mathbf{s}_1^t; \mathbf{s}_2^t; \dots; \mathbf{s}_K^t]$ represents the aggregated activation vectors from all participating clients. After forward propagation, the main server computes the loss function by comparing the predicted outputs and the true labels across all received samples.

d) *Server-side Backward Propagation*: Based on the computed loss, the main server executes backward propagation (BP), starting from the last layer, to obtain gradients of the trainable parameters in the server-side LoRA module. The LoRA parameters on the main server are then updated as follows:

$$\Delta \mathbf{W}_s^t \leftarrow \Delta \mathbf{W}_s^{t-1} - \gamma_s \mathbf{G}_s^t, \quad (5)$$

where \mathbf{G}_s^t represents the gradient of trainable parameters at the t -th training step, and γ_s is the learning rate of the server-side model.

e) *Downloading of Activation Vector Gradients*: After completing the BP process, the main server transmits the gradient values of the activation vectors with respect to each client's trainable parameters, $\frac{\partial \mathbf{s}_k^t}{\partial \Delta \mathbf{W}_{c,k}^t}$, to the corresponding client over the wireless network.

f) *Client-side Backward Propagation*: Each client then performs backward propagation to fine-tune its local trainable parameters based on the received gradients of the activation vectors. The update rule for the k -th client at the t -th training step is given by:

$$\Delta \mathbf{W}_k^t \leftarrow \Delta \mathbf{W}_k^{t-1} - \gamma_c \mathbf{G}_k^t, \quad (6)$$

where \mathbf{G}_k^t represents the gradient of the trainable parameters on the client side at the t -th training step, and γ_c is the learning rate for the client-side model.

B. Aggregation Phase

Once the clients and main server have completed I rounds of fine-tuning, the federated server enters the aggregation phase to aggregate and update the local models from all participating clients. This phase consists of the following three steps:

Algorithm 1: The FedsLLM Training Framework.

Input: $E, I, \gamma_c, \gamma_s, \mathbf{x}_k^t, y_k^t, \mathcal{K}, \mathbf{W}_c, \mathbf{W}_s, \mathcal{D}_k, \mathcal{D}$
Output: $\Delta \mathbf{W}_c^t, \Delta \mathbf{W}_s^t$

- 1 Initialize $\Delta \mathbf{W}_c^0, \Delta \mathbf{W}_s^0$
- 2 **for** $t = 1, 2, \dots, E$ **do**
 - // Runs on clients
 - 3 **foreach** $k \in \mathcal{K}$ **in parallel do**
 - 4 $\mathbf{s}_k^t = \varphi(\mathbf{W}_c | \Delta \mathbf{W}_{c,k}^{t-1}, \mathbf{x}_k^t)$
 - 5 Send (\mathbf{s}_k^t, y_k^t) to main server
 - 6 **end**
 - 7
 - // Runs on main server
 - 8 $\mathbf{S}^t = [\mathbf{s}_1^t; \mathbf{s}_2^t; \dots; \mathbf{s}_K^t]$
 - 9 $\hat{y}_k^t = \varphi(\mathbf{W}_s | \Delta \mathbf{W}_s^{t-1}, \mathbf{S}^t)$
 - 10 Calculate loss function value $F(\mathbf{W}_c, \Delta \mathbf{W}_c, \mathbf{W}_s, \Delta \mathbf{W}_s)$
 - 11 Calculate gradients of server-side model \mathbf{G}_s^t
 - 12 $\Delta \mathbf{W}_s^t \leftarrow \Delta \mathbf{W}_s^{t-1} - \gamma_s \mathbf{G}_s^t$
 - 13 Broadcast aggregated activations' gradients $\frac{\partial s_k^t}{\partial \Delta \mathbf{W}_{c,k}^t}$ to all clients
 - 14
 - // Runs on clients
 - 15 **foreach** $k \in \mathcal{K}$ **in parallel do**
 - 16 Calculate gradients of client-side model \mathbf{G}_k^t
 - 17 $\Delta \mathbf{W}_k^t \leftarrow \Delta \mathbf{W}_k^{t-1} - \gamma_c \mathbf{G}_k^t$
 - 18 **end**
 - 19
 - // Runs on fed server
 - 20 **if** $t \bmod I = 0$ **then**
 - 21 $\Delta \mathbf{W}_c^t = \sum_{k=1}^K \frac{|\mathcal{D}_k|}{|\mathcal{D}|} \Delta \mathbf{W}_k^t$
 - 22 Broadcast the new global client-side LoRA adapter $\Delta \mathbf{W}_c^t$ to all clients
 - 23 **end**
 - 24 **end**

a) *Uploading Client-side LoRA Module:* Each participating client uploads the trainable parameters of its client-side LoRA module to the federated server over the wireless network.

b) *Aggregation of Client-side LoRA Modules:* The federated server receives the LoRA modules from all clients and generates a new global client-side model by aggregating them, as described by the following equation:

$$\Delta \mathbf{W}_c^t = \sum_{k=1}^K \frac{|\mathcal{D}_k|}{|\mathcal{D}|} \Delta \mathbf{W}_k^t, \quad (7)$$

where $|\mathcal{D}_k|$ is the size of the local dataset at the k -th client, and $|\mathcal{D}| = \sum_{k=1}^K |\mathcal{D}_k|$ is the total number of data samples across all clients.

c) *Broadcasting the Global Client-side LoRA Module:* After the aggregation step, the federated server broadcasts the new global client LoRA module over the wireless network to all participating clients. Each client then updates its local LoRA module with the received global model, thus preparing for the next round of the fine-tuning phase.

The overall training framework for FedsLLM is outlined in Algorithm 1.

V. RESOURCE ALLOCATION FOR FEDSLLM

This section presents the mathematical modeling of the communication resource allocation problem in the FedsLLM framework, aimed at minimizing the training delay. Due to the varying local computing capabilities and dynamically changing communication resources of different clients, there are discrepancies in the training speed across clients. The presence of stragglers can significantly impact the overall training delay. Therefore, it is essential to balance the training delay among clients through efficient resource allocation to minimize the total training delay. Moreover, the split point of the model affects both the volume of activation vector data and the computational burden on the clients. Selecting an appropriate split point based on the environment can effectively optimize the training delay.

With the introduction of the LoRA module, both computation and communication data volume increase with the rank r . Within a certain range, the rank influences the convergence speed of the model. As the rank increases, the number of steps required to achieve the target model accuracy decreases, thus impacting the total training delay. Therefore, selecting an optimal rank is crucial for efficiently completing model training and reducing delay.

To this end, we propose an effective resource allocation algorithm that jointly optimizes split location selection, rank selection, subchannel allocation, and transmit power control to minimize the training delay of the FedsLLM framework.

A. Mathematical Model of Training Delay

To clearly define the resource variables to be allocated, we introduce the following:

- \mathbf{r} : $r_k^{i,s} \in \{0, 1\}$ and $r_k^{i,f} \in \{0, 1\}$ denote the subchannel allocation for wireless transmissions between the client and the main server, and between the client and the federated server, respectively. A value of $r_k^{i,s} = 1$ or $r_k^{i,f} = 1$ indicates that the i -th subchannel is assigned to client k , otherwise $r_k^{i,s} = 0$ or $r_k^{i,f} = 0$. The set of subchannels assigned to client k is represented as vectors $\mathbf{r}_k^s = [r_k^{1,s}, r_k^{2,s}, \dots, r_k^{M,s}]$ and $\mathbf{r}_k^f = [r_k^{1,f}, r_k^{2,f}, \dots, r_k^{N,f}]$, where M and N are the total number of subchannels between the client and the main server, and between the client and the federated server, respectively. Thus, $\mathbf{r}^s = [\mathbf{r}_1^s, \mathbf{r}_2^s, \dots, \mathbf{r}_K^s]$ and $\mathbf{r}^f = [\mathbf{r}_1^f, \mathbf{r}_2^f, \dots, \mathbf{r}_K^f]$ represent the sets of subchannel allocation decisions between the clients and the main and federated servers, respectively.
- \mathbf{p} : p_i^s denotes the transmission power spectral density (PSD) of the i -th subchannel when the client uploads to the main server. Similarly, p_i^f denotes the transmission PSD of the i -th subchannel when the client uploads local model parameters to the federated server. $\mathbf{p}^s = [p_1^s, p_2^s, \dots, p_M^s]$ and $\mathbf{p}^f = [p_1^f, p_2^f, \dots, p_N^f]$ represent the power control decisions for the subchannels between the client and the main and federated servers, respectively.
- $\boldsymbol{\mu}$: $\mu_j \in \{0, 1\}$ is the split location selection variable, where $\mu_j = 1$ indicates that the j -th layer is deployed on the client, while $\mu_j = 0$ indicates that it is deployed

on the main server. The vector $\boldsymbol{\mu} = [\mu_1, \mu_2, \dots, \mu_{\ell_c + \ell_s}]$ represents the selection of split locations.

- r : r denotes the rank of the LoRA module.

Split federated learning is performed over successive rounds of training until the model converges. Each complete forward and backward propagation process constitutes a local iteration round, which is sequentially executed by all participating clients and the main server. After I local iteration rounds, the clients upload their local model parameters to the federated server for aggregation, while the main server aggregates the local models from different clients to generate a new global model. This completes one global iteration round, and the model reaches convergence after E global rounds. For simplicity, we focus on analyzing a single local training round, and omit the index t for training rounds in the following discussion. The latency for transmitting activation vector gradients from the main server to the client and for broadcasting the global model by the federated server is negligible, due to the generally high transmission power of servers and the small size of transmitted data. The aggregation latency on both the federated server and the main server is also small and can be neglected due to the relatively low computation requirements and abundant server resources. Thus, we focus on the latency of the remaining six phases within a training round.

Assuming a pre-trained weight matrix $W \in \mathbb{R}^{d \times k}$, LoRA approximates the weight update as the product of two matrices via low rank decomposition: $W_0 + \Delta W = W_0 + BA$, where $A \in \mathbb{R}^{r \times k}$, $B \in \mathbb{R}^{d \times r}$, and the rank $r \ll \min(d, k)$. During training, W_0 remains frozen (no weights are updated), while A and B are the trainable weights. Consequently, the number of parameters added by the LoRA module is $r \times (d+k)$, which increases linearly with r .

1) *Clients Perform Forward Propagation*: In this phase, all clients perform FP in parallel. Let $\Phi_c^F(\boldsymbol{\mu}) = \sum_{j=1}^{\ell_c + \ell_s} \mu_j \rho_j$ denote the computational workload (in FLOPs) of the client's pre-trained model for processing each sample during the FP phase, where ρ_j represents the computational workload for the j -th layer of the pre-trained model. With the introduction of the LoRA module, the number of trainable parameters increases, and the computation workload also increases. Let $\Delta\Phi_c^F(\boldsymbol{\mu}, r) = \sum_{j=1}^{\ell_c + \ell_s} \mu_j r \Delta\rho_j$ denote the computational workload corresponding to the trainable parameters introduced by the LoRA module, where $\Delta\rho_j$ is the computational workload for the forward propagation of the trainable parameters at the j -th layer for each data sample per rank.

Each client randomly selects a mini-batch of b samples for processing during one round of forward propagation. The FP delay for client k can be expressed as:

$$T_k^F = \frac{b\kappa_k (\Phi_c^F(\boldsymbol{\mu}) + \Delta\Phi_c^F(\boldsymbol{\mu}, r))}{f_k}, \forall k \in \mathcal{K}, \quad (8)$$

where f_k denotes the computational capability of client k (i.e., the number of graphics processing unit (GPU) cycles per second), and κ_k is the number of GPU cycles required to complete a single floating-point operation on client k .

2) *Transmission of Activation Vectors*: After completing the forward propagation, each client sends the activation vector from the last layer to the main server over the wireless channel.

We consider a Frequency Division Multiple Access (FDMA) communication scenario. The activation vectors output by the LoRA module and the pre-training parameters are added and merged. Therefore, the size of activation vector data remains unchanged despite the introduction of the LoRA module. Let $\Gamma_s(\boldsymbol{\mu}) = \sum_{j=1}^{\ell_c + \ell_s} (\mu_j - \mu_{j+1}) \psi_j$ denote the data size of activation vectors in bits, where ψ_j is the data size for the activation vectors at the j -th layer of the pre-trained model. The uplink transmission rate from client k to the main server can be expressed as:

$$R_k^s = \sum_{i=1}^M r_k^{i,s} B_i^s \log_2 \left(1 + \frac{P_i^s G_c G_s \gamma(d_k^s)}{(\sigma^s)^2} \right), \forall k \in \mathcal{K}, \quad (9)$$

where B_i^s is the bandwidth allocated to the i -th subchannel between the client and the main server, G_c and G_s represent the effective antenna gains of the client and main server, $\gamma(d_k^s)$ is the average channel gain from client k to the main server, d_k^s is the communication distance between client k and the main server, and $(\sigma^s)^2$ is the PSD of the wireless channel noise. The activation vector transmission delay for client k can be expressed as:

$$T_k^s = \frac{b\Gamma_s(\boldsymbol{\mu})}{R_k^s}, \forall k \in \mathcal{K}. \quad (10)$$

3) *Main Server Performs Forward Propagation*: In this phase, the main server receives activation vectors from all participating clients and executes forward propagation. Let $\Phi_s^F(\boldsymbol{\mu}) = \sum_{j=1}^{\ell_c + \ell_s} (1 - \mu_j) \rho_j$ denote the computational workload of the main server's pre-trained model for processing activation vectors from one client, and $\Delta\Phi_s^F(\boldsymbol{\mu}, r) = \sum_{j=1}^{\ell_c + \ell_s} (1 - \mu_j) r \Delta\rho_j$ denote the computational workload corresponding to the trainable parameters. The main server utilizes the activation vectors uploaded by all participating clients to perform forward propagation. The forward propagation delay on the main server can be expressed as:

$$T_s^F = \frac{Kb\kappa_s (\Phi_s^F(\boldsymbol{\mu}) + \Delta\Phi_s^F(\boldsymbol{\mu}, r))}{f_s}, \quad (11)$$

where f_s denotes the computational capability of the main server, and κ_s denotes the number of GPU cycles required by the main server to complete a single floating-point operation.

4) *Main Server Performs Backward Propagation*: After completing forward propagation, the main server begins backward propagation. Let $\Phi_s^B(\boldsymbol{\mu}) = \sum_{j=1}^{\ell_c + \ell_s} (1 - \mu_j) \varpi_j$ represent the total computational workload for backward propagation of the pre-trained parameters for each data sample, where ϖ_j is the computational workload corresponding to the j -th layer neural network. Let $\Delta\Phi_s^B(\boldsymbol{\mu}, r) = \sum_{j=1}^{\ell_c + \ell_s} (1 - \mu_j) r \Delta\varpi_j$ represent the total computational workload for backward propagation of the trainable parameters in the main server, where $\Delta\varpi_j$ is the computational workload for trainable parameters of each data sample for each rank at the j -th layer. The backward propagation delay on the main server can be expressed as:

$$T_s^B = \frac{Kb\kappa_s (\Phi_s^B(\boldsymbol{\mu}) + \Delta\Phi_s^B(\boldsymbol{\mu}, r))}{f_s}. \quad (12)$$

5) *Client Performs Backward Propagation*: In this stage, each client receives the gradient of the activation vector and performs the backward propagation process. Let $\Phi_c^B(\boldsymbol{\mu}) = \sum_{j=1}^{\ell_c+\ell_s} \mu_j \varpi_j$ denote the total computational workload for the client's pre-trained parameters during backward propagation for each data sample. Let $\Delta\Phi_c^B(\boldsymbol{\mu}, r) = \sum_{j=1}^{\ell_c+\ell_s} \mu_j r \Delta\varpi_j$ represent the computational workload associated with the trainable parameters. The backward propagation delay for client k can be expressed as:

$$T_k^B = \frac{b\kappa_k (\Phi_c^B(\boldsymbol{\mu}) + \Delta\Phi_c^B(\boldsymbol{\mu}, r))}{f_k}, \forall k \in \mathcal{K}. \quad (13)$$

6) *Client Local Model Upload*: After completing I rounds of local iterations, the client and the main server aggregate their local models to update the global model. Some parameters are aggregated on the main server, while all the trainable parameters from the client-side model are uploaded to the federated server for aggregation. The updated global model parameters are then broadcast by the federated server to all clients to begin the next round of global iterations. Since the number of trainable parameters is linearly related to the rank r , let $\Delta\Theta_c(\boldsymbol{\mu}, r) = \sum_{j=1}^{\ell_c+\ell_s} \mu_j r \Delta\xi_j$ represent the total data volume of the client-side trainable parameters. Here, $\Delta\xi_j$ denotes the data volume corresponding to the trainable parameters for each rank at the j -th layer.

The uplink transmission rate from client k to the federated server is given by:

$$R_k^f = \sum_{i=1}^N r_k^{i,f} B_i^f \log_2 \left(1 + \frac{p_i^f G_c G_f \gamma(d_k^f)}{(\sigma^f)^2} \right), \forall k \in \mathcal{K}, \quad (14)$$

where B_i^f is the bandwidth allocated to the i -th subchannel between the client and the federated server, G_f denotes the effective antenna gain of the federated server, $\gamma(d_k^f)$ is the average channel gain from client k to the federated server, d_k^f is the communication distance between client k and the federated server, and $(\sigma^f)^2$ represents the PSD of the noise in the wireless channel.

The transmission delay for client k to upload the local model parameters to the federated server can be expressed as:

$$T_k^f = \frac{\Delta\Theta_c(\boldsymbol{\mu}, r)}{R_k^f}, \forall k \in \mathcal{K}. \quad (15)$$

B. Resource Allocation Problem Formulation

As illustrated in Fig. 2, the total latency of a local training round can be expressed as:

$$T_{local}(\mathbf{r}^s, \mathbf{r}^f, \mathbf{p}^s, \mathbf{p}^f, \boldsymbol{\mu}, r) = \max_k \{T_k^F + T_k^S\} + T_s^F + T_s^B + \max_k \{T_k^B\}. \quad (16)$$

The total delay for the entire training process can be written as:

$$T(\mathbf{r}^s, \mathbf{r}^f, \mathbf{p}^s, \mathbf{p}^f, \boldsymbol{\mu}, r) = E(r)(IT_{local} + \max_k \{T_k^f\}), \quad (17)$$

where $E(r)$ represents the number of global iteration rounds required to achieve the target accuracy, which varies with different values of rank r .

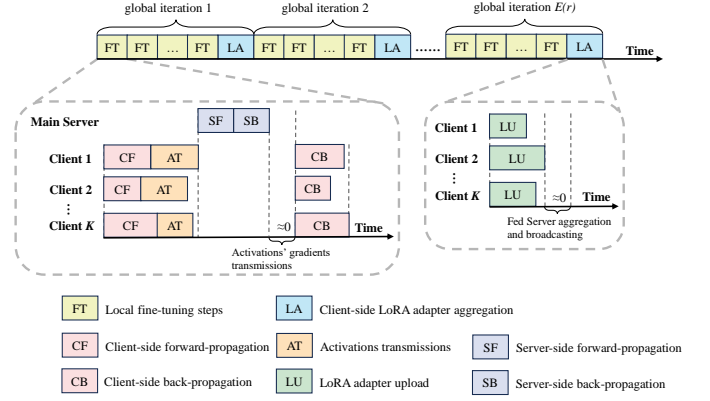


Fig. 2. Illustration of FedSLLM training procedure.

Time-varying and heterogeneous wireless channel conditions, as well as varying client computational capabilities, can result in severe dropout issues. Additionally, the choice of split location has a significant impact on both computation and communication latency. Therefore, proper allocation of communication resources is crucial to accelerating the training process. Based on these observations, we formulate the following problem aimed at minimizing the training delay:

$$\begin{aligned} \mathcal{P}: \quad & \min_{\mathbf{r}^s, \mathbf{r}^f, \mathbf{p}^s, \mathbf{p}^f, \boldsymbol{\mu}, r} T & (18) \\ & \text{s.t. C1: } r_k^{i_1, s} \in \{0, 1\}, r_k^{i_2, f} \in \{0, 1\}, \quad \forall k \in \mathcal{K}, \\ & i_1 = 1, 2, \dots, M, i_2 = 1, 2, \dots, N, \\ & \text{C2: } \sum_{k=1}^K r_k^{i_1, s} = 1, \sum_{k=1}^K r_k^{i_2, f} = 1, \quad i_1 = 1, 2, \dots, M, \\ & i_2 = 1, 2, \dots, N, \\ & \text{C3: } \mu_j \in \{0, 1\}, \mu_j \geq \mu_{j+1}, \quad j = 1, 2, \dots, \ell_c + \ell_s, \\ & \text{C4: } \sum_{i=1}^M r_k^{i, s} p_i^s B_i^s \leq p_k^{\max}, \sum_{i=1}^N r_k^{i, f} p_i^f B_i^f \leq p_k^{\max}, \forall k \in \mathcal{K}, \\ & \text{C5: } \sum_{i=1}^M \sum_{k=1}^K r_k^{i, s} p_i^s B_i^s \leq p_{th}^s, \sum_{i=1}^N \sum_{k=1}^K r_k^{i, f} p_i^f B_i^f \leq p_{th}^f, \\ & \text{C6: } p_{i_1}^s \geq 0, p_{i_2}^f \geq 0, i_1 = 1, 2, \dots, M, i_2 = 1, 2, \dots, N, \\ & \text{C7: } r \in \mathbb{Z}^+. \end{aligned}$$

Constraints C1 and C2 ensure that each subchannel is assigned to only one edge device, thereby avoiding co-channel interference. Constraint C3 guarantees the uniqueness of the split location selection. Constraint C4 imposes a transmit power limit for each client, while C5 defines the total uplink transmit power limit with thresholds p_{th}^s and p_{th}^f . Constraint C6 ensures that the transmit power of each subchannel is non-negative, and C7 ensures that the rank is a positive integer.

VI. SOLUTION APPROACH

To solve the problem in (18), we first fix the other decision variables and focus on subchannel assignment. The resulting

Algorithm 2: Greedy Subchannel Allocation Approach.

Input: $\mathcal{K}, B_i^s, B_i^f, f_k, d_k^f$
Output: $\mathbf{r}^{s*}, \mathbf{r}^{f*}$

- 1 **Initialization:** Set $\mathbf{r}^s, \mathbf{r}^f \leftarrow 0$
- 2 The set of remaining clients $\mathcal{A}_s, \mathcal{A}_f \leftarrow \mathcal{K}$
- 3 The set of subchannels to be allocated
 $\mathcal{M} \leftarrow \{1, 2, \dots, M\}, \mathcal{N} \leftarrow \{1, 2, \dots, N\}$.
- 4 **Phase 1: Ensure Each Client Receives at Least One Subchannel**
- 5 **for** $j = 1, 2, \dots, K$ **do**
- 6 Find $n \leftarrow \arg \min_{k \in \mathcal{A}_s} \{f_k\}, m \leftarrow \arg \max_{i \in \mathcal{M}} \{B_i^s\}$
- 7 Let $r_n^{m,s} \leftarrow 1, \mathcal{A}_s \leftarrow \mathcal{A}_s - \{n\}, \mathcal{M} \leftarrow \mathcal{M} - \{m\}$
- 8 Find $n \leftarrow \arg \max_{k \in \mathcal{A}_f} \{d_k^f\}, m \leftarrow \arg \max_{i \in \mathcal{N}} \{B_i^f\}$
- 9 Let $r_n^{m,f} \leftarrow 1, \mathcal{A}_f \leftarrow \mathcal{A}_f - \{n\}, \mathcal{N} \leftarrow \mathcal{N} - \{m\}$
- 10 **end**
- 11 **Phase 2: Allocate Remaining Subchannels**
- 12 $\mathcal{A}_s, \mathcal{A}_f \leftarrow \mathcal{K}$
- 13 **while** $\mathcal{M} \neq \emptyset$ **do**
- 14 Find $n \leftarrow \arg \max_{i \in \mathcal{A}_s} \{T_k^F + T_k^s\},$
 $m \leftarrow \arg \max_{i \in \mathcal{M}} \{B_i^s\}$
- 15 **if** r_n *does not meet C4 or C5 in (18)* **then**
- 16 $\mathcal{A}_s \leftarrow \mathcal{A}_s - \{n\}$
- 17 **end**
- 18 **else**
- 19 $r_n^m \leftarrow 1, \text{Update } T_k^s, \mathcal{M} \leftarrow \mathcal{M} - \{m\}$
- 20 **end**
- 21 **end**
- 22 **while** $\mathcal{N} \neq \emptyset$ **do**
- 23 Find $n \leftarrow \arg \max_{i \in \mathcal{A}_f} \{T_k^f\}, m \leftarrow \arg \max_{i \in \mathcal{N}} \{B_i^f\}$
- 24 **if** r_n *does not meet C4 or C5 in (18)* **then**
- 25 $\mathcal{A}_f \leftarrow \mathcal{A}_f - \{n\}$
- 26 **end**
- 27 **else**
- 28 $r_n^m \leftarrow 1, \text{Update } T_k^f, \mathcal{N} \leftarrow \mathcal{N} - \{m\}$
- 29 **end**
- 30 **end**

subproblem can be represented as:

$$\begin{aligned} P1 : \min_{\mathbf{r}^s, \mathbf{r}^f} T \\ \text{s.t. C1, C2, C4, C5.} \end{aligned} \quad (19)$$

Problem (19) has a non-convex optimization objective and includes integer-type optimization variables, making it challenging to find the optimal solution directly. Since the objective function of problem (19) is determined by the dropout with the longest latency during the client's upload to the main server or the federated server, minimizing the training latency requires prioritizing the allocation of subchannels to clients with longer latency. To achieve this, we design a subchannel allocation method based on a greedy algorithm. The core idea is to allocate subchannels with faster transmission rates to clients with weaker computational and communication capabilities first. After each client is assigned a channel, the remaining free channels are allocated to lagging clients in each iteration until all subchannels are assigned. The process of subchannel allocation using the greedy algorithm is described in detail in Algorithm 2.

After completing the subchannel assignment for each client, we introduce auxiliary variables $p_{k,\xi}^s$ and $p_{k,\xi}^f$ to represent

the transmission PSD of the ξ -th subchannel assigned to client k for uploading data to the main server and federated server, respectively. Similarly, auxiliary variables $B_{k,\xi}^s$ and $B_{k,\xi}^f$ denote the bandwidth of the ξ -th subchannel allocated to client k for uploading data to the main server and the federated server, respectively. After fixing the decision variables \mathbf{r}^s and \mathbf{r}^f , the problem in (18) can be expressed as:

$$\begin{aligned} \min_{\mathbf{p}^s, \mathbf{p}^f, \boldsymbol{\mu}, r} T \quad (20) \\ \text{s.t. C3} \\ \tilde{\text{C4}} : \sum_{\xi=1}^{M_k} p_{k,\xi}^s B_{k,\xi}^s \leq p_k^{\max}, \sum_{\xi=1}^{N_k} p_{k,\xi}^f B_{k,\xi}^f \leq p_k^{\max}, \quad \forall k \in \mathcal{K}, \\ \tilde{\text{C5}} : \sum_{k=1}^K \sum_{\xi=1}^{M_k} p_{k,\xi}^s B_{k,\xi}^s \leq p_{th}^s, \sum_{k=1}^K \sum_{\xi=1}^{N_k} p_{k,\xi}^f B_{k,\xi}^f \leq p_{th}^f, \\ \tilde{\text{C6}} : p_{k,\xi_1}^s \geq 0, p_{k,\xi_2}^f \geq 0, \quad \forall k \in \mathcal{K}, \xi_1 = 1, 2, \dots, M_k, \\ \xi_2 = 1, 2, \dots, N_k, \\ \text{C7} : r \in \mathbb{Z}^+, \end{aligned}$$

where M_k and N_k represent the number of subchannels allocated to client k for communication with the main and federated servers, respectively.

The objective function of problem (20) is non-convex, which complicates finding the optimal solution. To address this, we introduce auxiliary variables T_1, T_2 , and T_3 , which satisfy $T_1 \geq \max_k \{T_k^F + T_k^s\}$, $T_2 \geq \max_k \{T_k^B\}$, and $T_3 \geq \max_k \{T_k^f\}$. This allows the problem in (20) to be transformed into:

$$\begin{aligned} \min_{\mathbf{p}^s, \mathbf{p}^f, \boldsymbol{\mu}, r, T_1, T_2, T_3} \tilde{T} \quad (21) \\ \text{s.t. C3, } \tilde{\text{C4}}, \tilde{\text{C5}}, \tilde{\text{C6}}, \text{C7} \\ \text{C8} : \frac{b\kappa_k(\Phi_c^F(\boldsymbol{\mu}) + \Delta\Phi_c^F(\boldsymbol{\mu}, r))}{f_k} \\ + \frac{b\Gamma_s(\boldsymbol{\mu})}{\sum_{\xi=1}^{M_k} B_{k,\xi}^s \log_2 \left(1 + \frac{p_{k,\xi}^s G_c G_s \gamma(d_k^s)}{(\sigma^s)^2} \right)} \leq T_1, \quad \forall k \in \mathcal{K}, \\ \text{C9} : \frac{b\kappa_k(\Phi_c^B(\boldsymbol{\mu}) + \Delta\Phi_c^B(\boldsymbol{\mu}, r))}{f_k} \leq T_2, \quad \forall k \in \mathcal{K}, \\ \text{C10} : \frac{\Delta\Theta_c(\boldsymbol{\mu}, r)}{\sum_{\xi=1}^{N_k} B_{k,\xi}^f \log_2 \left(1 + \frac{p_{k,\xi}^f G_c G_f \gamma(d_k^f)}{(\sigma^f)^2} \right)} \leq T_3, \quad \forall k \in \mathcal{K}, \end{aligned}$$

where $\tilde{T}(\mathbf{p}^s, \mathbf{p}^f, \boldsymbol{\mu}, r, T_1, T_2, T_3) = E(r)(I(T_1 + T_s^F + T_s^B + T_2) + T_3)$.

In order to minimize \tilde{T} , we need to determine the values of T_1, T_2 , and T_3 . The optimal solution from problem (21) must satisfy $T_1 = \max_k \{T_k^F + T_k^s\}$, $T_2 = \max_k \{T_k^B\}$, and $T_3 = \max_k \{T_k^f\}$, ensuring that the transformed problem in (21) is equivalent to the original problem in (20). The non-convexity of constraints C8 and C10 makes the problem challenging to solve directly. To handle this, we introduce two sets of auxiliary variables $\boldsymbol{\theta}^s = \{\theta_{1,1}^s, \theta_{1,2}^s, \dots, \theta_{K,M_K}^s\}$ and $\boldsymbol{\theta}^f =$

$\{\theta_{1,1}^f, \theta_{1,2}^f, \dots, \theta_{K,N_K}^f\}$, which can be expressed as:

$$\theta_{k,\xi}^s = B_{k,\xi}^s \log_2 \left(1 + \frac{p_{k,\xi}^s G_c G_s \gamma(d_k^s)}{(\sigma^s)^2} \right), \quad (22)$$

$$\theta_{k,\xi}^f = B_{k,\xi}^f \log_2 \left(1 + \frac{p_{k,\xi}^f G_c G_f \gamma(d_k^f)}{(\sigma^f)^2} \right). \quad (23)$$

By substituting the auxiliary variables $\theta^s = \{\theta_{1,1}^s, \theta_{1,2}^s, \dots, \theta_{K,M_K}^s\}$ and $\theta^f = \{\theta_{1,1}^f, \theta_{1,2}^f, \dots, \theta_{K,N_K}^f\}$ into the problem (21), the transformed problem can be represented as:

$$\begin{aligned} & \min_{\theta^s, \theta^f, \mu, r, T_1, T_2, T_3} \tilde{T} \\ & \text{s.t. C3, C7, C9} \end{aligned} \quad (24)$$

$$\hat{\text{C4}} : \sum_{\xi=1}^{M_k} \sigma_s^2 B_{k,\xi}^s \frac{2^{\frac{\theta_{k,\xi}^s}{B_{k,\xi}^s}} - 1}{G_c G_s \gamma(d_k^s)} \leq p_k^{\max}, \sum_{\xi=1}^{N_k} \sigma_f^2 B_{k,\xi}^f \frac{2^{\frac{\theta_{k,\xi}^f}{B_{k,\xi}^f}} - 1}{G_c G_f \gamma(d_k^f)} \leq p_k^{\max}, \quad \forall k \in \mathcal{K},$$

$$\hat{\text{C5}} : \sum_{k=1}^K \sum_{\xi=1}^{M_k} \sigma_s^2 B_{k,\xi}^s \frac{2^{\frac{\theta_{k,\xi}^s}{B_{k,\xi}^s}} - 1}{G_c G_s \gamma(d_k^s)} \leq p_{th}^s,$$

$$\sum_{k=1}^K \sum_{\xi=1}^{N_k} \sigma_f^2 B_{k,\xi}^f \frac{2^{\frac{\theta_{k,\xi}^f}{B_{k,\xi}^f}} - 1}{G_c G_f \gamma(d_k^f)} \leq p_{th}^f,$$

$$\hat{\text{C6}} : \theta_{k,\xi_1}^f \geq 0, \theta_{k,\xi_2}^f \geq 0, \quad \forall k \in \mathcal{K}, \xi_1 = 1, 2, \dots, M_k, \xi_2 = 1, 2, \dots, N_k,$$

$$\hat{\text{C8}} : \frac{b\kappa_k(\Phi_c^F(\mu) + \Delta\Phi_c^F(\mu, r))}{f_k} + \frac{b\Gamma_s(\mu)}{\sum_{\xi=1}^{M_k} \theta_{k,\xi}^s} \leq T_1, \quad \forall k \in \mathcal{K},$$

$$\hat{\text{C10}} : \frac{\Delta\Theta_c(\mu, r)}{\sum_{\xi=1}^{N_k} \theta_{k,\xi}^f} \leq T_3, \quad \forall k \in \mathcal{K},$$

We observe that if the decision variables μ and r are fixed, the optimization problem (24) can be simplified as follows:

$$\begin{aligned} \mathcal{P2} : & \min_{\theta^s, \theta^f, T_1, T_2, T_3} \tilde{T} \\ & \text{s.t. } \hat{\text{C4}}, \hat{\text{C5}}, \hat{\text{C6}}, \hat{\text{C8}}, \text{C9}, \hat{\text{C10}}. \end{aligned} \quad (25)$$

Problem (25) is a convex optimization problem, which can be efficiently solved using standard optimization toolkits such as CVX.

Similarly, if the decision variables θ^s , θ^f , r , T_1 , T_2 , and T_3 are fixed, the original problem (24) reduces to:

$$\begin{aligned} \mathcal{P3} : & \min_{\mu} \tilde{T} \\ & \text{s.t. } \text{C8}, \hat{\text{C9}}, \text{C10}. \end{aligned} \quad (26)$$

Problem (26) is a mixed-integer linear programming (MILP) problem. The number of possible split locations represented by μ corresponds to the number of layers in the neural network, which is typically small. Therefore, an exhaustive search can be efficiently employed to solve this problem.

Algorithm 3: BCD-Based Algorithm for Minimizing Training Delay.

Input: convergence tolerance ϵ , maximum iterations

τ_{\max}

Output: $\mathbf{r}^{s*}, \mathbf{r}^{f*}, \mathbf{p}^{s*}, \mathbf{p}^{f*}, \mu^*, r^*$

1 **Initialization:** $\theta^{s,0}, \theta^{f,0}, \mu^0, r^0, T_1^0, T_2^0, T_3^0$

2 set iteration index $\tau = 0$

3 **repeat**

4 $\tau \leftarrow \tau + 1$

5 Solve $\mathcal{P1}$ based on Algorithm 2 to obtain $\mathbf{r}^{s,\tau}, \mathbf{r}^{f,\tau}$

6 Solve $\mathcal{P2}$ with convex optimization tools to obtain $\theta^{s,\tau}, \theta^{f,\tau}, T_1^\tau, T_2^\tau, T_3^\tau$

7 Solve $\mathcal{P3}$ using exhaustive search to update μ^τ

8 Solve $\mathcal{P4}$ with exhaustive search to update r^τ

9 **until** $|\tilde{T}^\tau - \tilde{T}^{\tau-1}| \leq \epsilon$ or $\tau = \tau_{\max}$

10 **return** $\mathbf{r}^{s*}, \mathbf{r}^{f*}, \mathbf{p}^{s*}, \mathbf{p}^{f*}, \mu^*, r^*$

By fixing the decision variables θ^s , θ^f , μ , T_1 , T_2 , and T_3 , the original problem (24) simplifies further to:

$$\begin{aligned} \mathcal{P4} : & \min_r \tilde{T} \\ & \text{s.t. } \text{C7}, \hat{\text{C8}}, \text{C9}, \hat{\text{C10}}, \end{aligned} \quad (27)$$

where the number of global iterations $E(r)$ can be estimated offline by pre-training on a small dataset. Problem (27) is also an MILP problem, and the rank r of the LoRA module typically takes integer values within a small predefined range. Thus, we apply an exhaustive search to find the optimal value of r .

As discussed above, we decompose the original optimization problem (18) into four independent subproblems (i.e., $\mathcal{P1}$, $\mathcal{P2}$, $\mathcal{P3}$, and $\mathcal{P4}$), each of which can be solved individually. Based on these analyses, we propose a Block-Coordinate Descent (BCD)-based algorithm using an alternating optimization strategy to solve problem (18). The detailed steps of this algorithm are presented in Algorithm 3. Since the original problem (18) is non-convex and mixed-integer, theoretical convergence guarantees for the proposed BCD-based algorithm are difficult to provide. Nevertheless, extensive practical experiments demonstrate that the algorithm consistently converges rapidly to a stable and efficient solution after a finite number of iterations, regardless of the initial conditions.

VII. PERFORMANCE EVALUATION

In this section, we present numerical results to evaluate the learning performance of the proposed FedLLM framework, as well as the effectiveness of the proposed rank selection and resource allocation strategies.

A. Simulation Setup

In our simulations, we consider K clients uniformly distributed within a circular region with radius $d_{\max} = 20\text{m}$, with the federated server located at the center, and the main server placed 100m away from the centroid. Unless otherwise specified, we set the default number of clients K to 5. The

computational capability of the clients is uniformly distributed within the range $[1, 1.6] \times 10^9$ cycles/s, while the computational capability of the main server is fixed at 5×10^9 cycles/s.

The total bandwidth available for communication between each client and both the federated server and the main server is set to 500 kHz, with all subchannels equally sharing this bandwidth. The PSD of noise is set to -174 dBm/Hz [41], and the maximum transmit power for all clients is set to 41.76 dBm. All clients have the same computing intensity of $\frac{1}{1024}$ cycles per FLOP, whereas the computing intensity of the main server is set to $\frac{1}{32768}$ cycles per FLOP.

The path loss model is given by $128.1 + 37.6 \log_{10}(d)$ (where distance d is measured in km), with a shadow fading standard deviation of 8dB. For convenience, the detailed simulation parameters are summarized in Table II.

TABLE II
SIMULATION PARAMETERS

Parameter	Value	Parameter	Value
f_s	5×10^9 cycles/s	f_k	$[1, 1.6] \times 10^9$ cycles/s
K	5	M, N	20
η_c, η_s	4×10^{-4}	$G_c G_s$	160
$G_c G_f$	80	b	16
κ_s	$\frac{1}{32768}$ cycles/FLOPs	κ_k	$\frac{1}{1024}$ cycles/FLOPs
d_{\max}	20 m	B_c, B_s	500 kHz
p_k^{\max}	41.76 dBm	$p_{\text{th}}^s, p_{\text{th}}^f$	46.99 dBm
σ_s^2, σ_f^2	-174 dBm/Hz		

We evaluate the performance of FedsLLM on a natural language generation task using the E2E dataset [19]. The E2E dataset consists of restaurant-domain data, including approximately 42,000 training samples, 4,600 validation samples, and 4,600 test samples. For the language modeling task, we adopt the GPT-2 model architecture [18], which primarily consists of an embedding layer, Transformer decoder blocks, and a language modeling head. We use the smallest variant in the GPT-2 family, GPT-2 small (GPT2-S), which comprises 12 Transformer decoder layers and approximately 124 million parameters. Detailed network parameters and computational complexity for GPT2-S are provided in Table III. In the simulations, the computation of backpropagation is estimated as twice that of forward propagation, while the computational workload of the token embedding and positional encoding layers is negligible since they are implemented by simple table lookups.

By default, for GPT2-S, we set the mini-batch size to 16, the learning rate to 0.0004, and the maximum sequence length to 512. Similarly, for GPT2-M, the batch size is set to 12, with the same learning rate and sequence length. The LoRA modules are applied to fine-tune the Query (Q) and Value (V) components of all Transformer blocks.

B. Performance Evaluation

To demonstrate the advantages of the proposed FedsLLM framework, we compare it with a centralized LoRA fine-tuning approach. In the centralized baseline, the server collects raw data directly from participating clients and performs centralized fine-tuning using LoRA modules.

TABLE III
COMPUTATIONAL COMPLEXITY ANALYSIS OF GPT2-S WITH LoRA

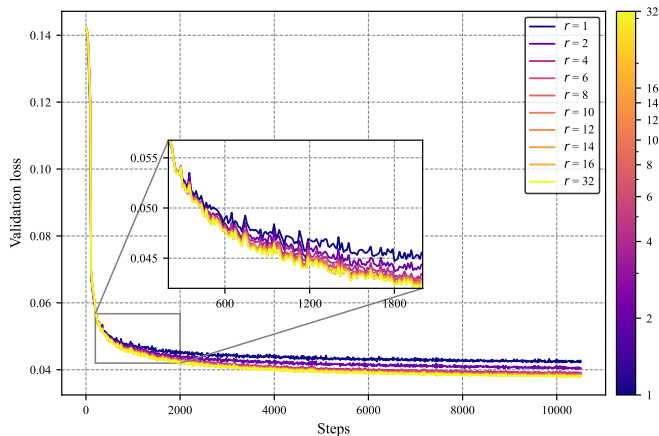
Component	Parameters	FLOPs (GFLOP)
Token Embedding	38.6M	–
Position Encoding	0.786M	–
Transformer Block $\times 12$		
LayerNorm	1.5K	0.025
Multi-Head Attention	2.36M	257.7
LoRA Adapter (per rank)	1.5K	0.050
Feed-Forward	4.72M	309.2
Final LayerNorm	1.5K	0.025
LM Head	–	1264.1

1) *Convergence Rate*: Fig. 3 illustrates the convergence behavior of both FedsLLM and centralized training schemes on the E2E dataset, using the GPT2-S and GPT2-M models for the natural language generation task. We evaluate model performance on the validation set every 12 training steps. The convergence speed generally increases with higher LoRA rank values, although the improvement becomes less significant as the rank continues to increase. This phenomenon arises because different rank values correspond to varying numbers of trainable parameters, thereby affecting model fitting capability. In general, fewer steps are required to reach a given target accuracy with higher ranks; however, due to the stochastic nature of the training process, smaller ranks occasionally achieve certain accuracy levels in fewer steps. Specifically, as shown in Fig. 4, the overall number of steps required to achieve a target accuracy tends to increase as the target accuracy rises and as the LoRA rank decreases. Since the rank value significantly impacts computational cost, communication overhead, and convergence steps, selecting an appropriate LoRA rank is critical to minimize the total training delay.

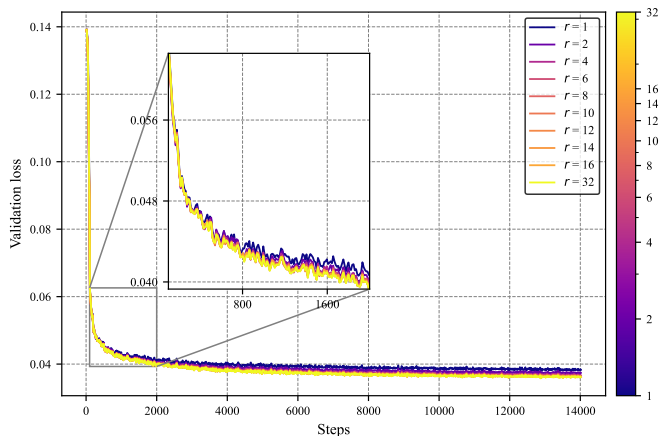
2) *Converged Accuracy*: Table IV presents a comparison of the converged accuracy between FedsLLM and the centralized training method for fine-tuning GPT2-S on the E2E dataset for the natural language generation task, using Perplexity (PPL) as the performance metric. FedsLLM achieves comparable performance, with the largest PPL difference across different rank values being only 0.001. This result can be attributed to the model splitting in FedsLLM, where the server-side model is trained jointly on data from all participating clients, while the client-side model is trained on local data. This approach is more resilient to data heterogeneity. Furthermore, as the rank increases, both FedsLLM and the centralized training method show improved test accuracy and lower PPL. The increase in the number of trainable parameters enhances the model’s fitting ability, allowing it to better adapt to downstream tasks based on the language comprehension capabilities of the pre-trained model.

C. Performance Evaluation of the Proposed Resource Management Strategy

In this subsection, we evaluate the effectiveness of the proposed resource allocation and rank selection strategy in



(a) Validation loss with GPT2-S.



(b) Validation loss with GPT2-M.

Fig. 3. Validation loss of FedLLM and centralized training on the E2E dataset with GPT2-S and GPT2-M under different LoRA ranks.

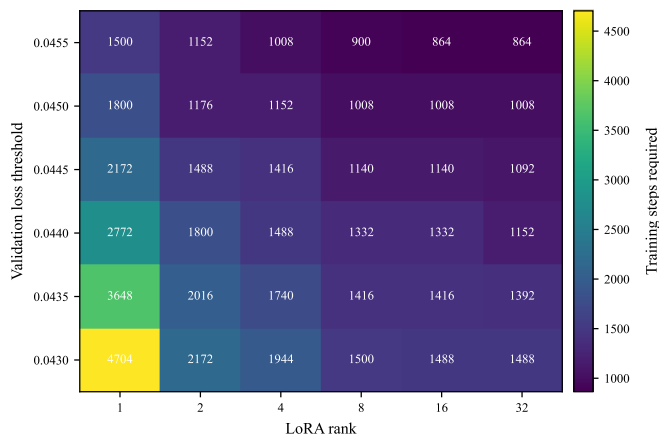


Fig. 4. Number of steps required to reach target loss values under different LoRA ranks.

reducing the total latency by comparing it with the following four baselines:

- **Baseline a:** Randomized average allocation of subchannels with uniform subchannel transmit PSD on the client side, and randomized split location and rank selection.

TABLE IV
CONVERGED TEST PERPLEXITY FOR E2E

Learning Framework	Rank				
	1	2	4	6	8
Centralized	1.0424	1.0407	1.0393	1.0388	1.0385
FedLLM	1.0433	1.0413	1.0399	1.0398	1.0392

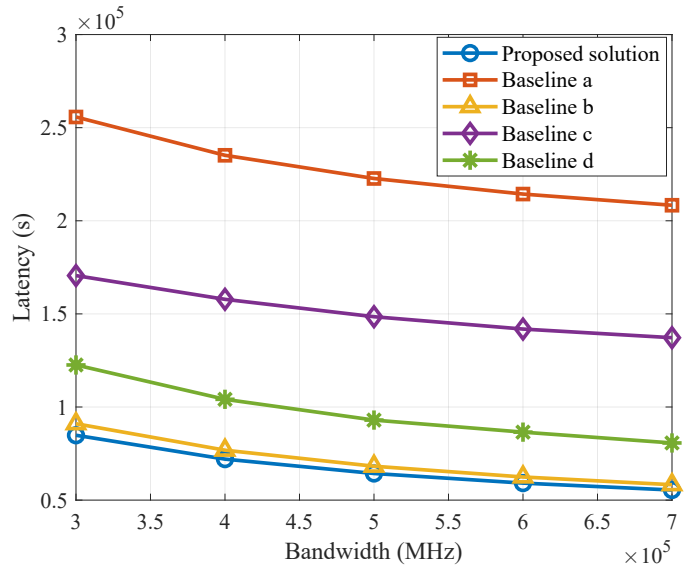


Fig. 5. Latency versus total bandwidth of each client.

- **Baseline b:** Randomized average allocation of subchannels, uniform subchannel transmit PSD on the client side, and the proposed rank and split location selection schemes.
- **Baseline c:** Randomized split location selection using the proposed greedy subchannel assignment, power control, and rank selection scheme.
- **Baseline d:** The proposed greedy subchannel assignment, power control, and split location selection scheme with random rank selection.

Fig. 5 illustrates the total delay versus total bandwidth performance. The proposed resource allocation scheme significantly reduces latency by approximately 60% compared to the unoptimized baseline a. It is evident that latency decreases as the total bandwidth increases, which can be attributed to the improved uplink communication speed between the client and both the federated and main servers. As total bandwidth increases, the data communication delay decreases, and the reduction in delay due to optimized subchannel allocation and power control slows down, with total delay becoming more determined by computational delays. Consequently, the performance gap between the proposed solution and baseline b gradually narrows. Additionally, we observe a substantial reduction in delay with the proposed solution compared to baseline d, which uses random rank selection. This highlights the importance of optimized rank selection in improving performance.

Fig. 6 illustrates how latency varies with the number of floating-point operations that the client can complete per

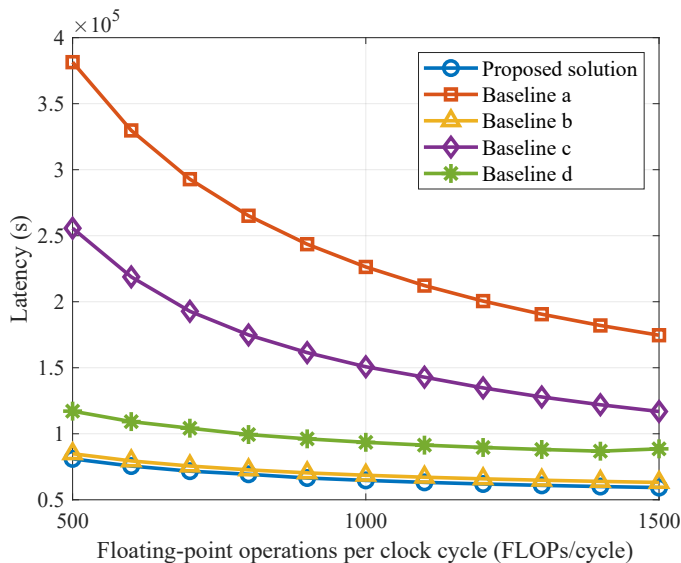


Fig. 6. The effect of LoRA rank on the number of steps required to reach the target loss value.

GPU cycle. The number of floating-point operations per cycle is directly related to the number of cores in the client's GPU; more cores allow for more floating-point operations to be processed in parallel during each cycle. The latency of all schemes decreases as the number of floating-point operations per GPU cycle increases, reflecting the increased computational capability and reduced computational latency of the client. The proposed solution achieves the lowest latency among all schemes. Additionally, it can be observed that the latency gap between baseline c (unoptimized split location) and the proposed solution gradually narrows. This is because the split location mainly affects the computational workload of the client, which in turn impacts computational latency. As the client's computational capability increases, the impact of computational latency on the total latency becomes less significant.

Fig. 7 demonstrates the relationship between latency and the computational capability of the main server. The proposed solution consistently achieves the lowest latency, with training latency decreasing as the computational capability of the main server increases. The significant increase in latency for baseline d compared to baseline b illustrates that optimizing the rank has a greater impact on performance than optimizing communication settings in this scenario. Furthermore, it is observed that the performance improvement from optimizing power control and subchannel assignment increases as the main server's computational capability grows. This is because the computational delay in total latency decreases, and communication conditions begin to play a more significant role in determining the total delay.

Fig. 8 shows how delay varies with the maximum transmit power of the client's uplink to both the main and federated servers. As the maximum transmit power increases, the delay decreases, reflecting the faster communication speed enabled by the increased client transmit power. The proposed scheme significantly reduces training delay compared to the baseline

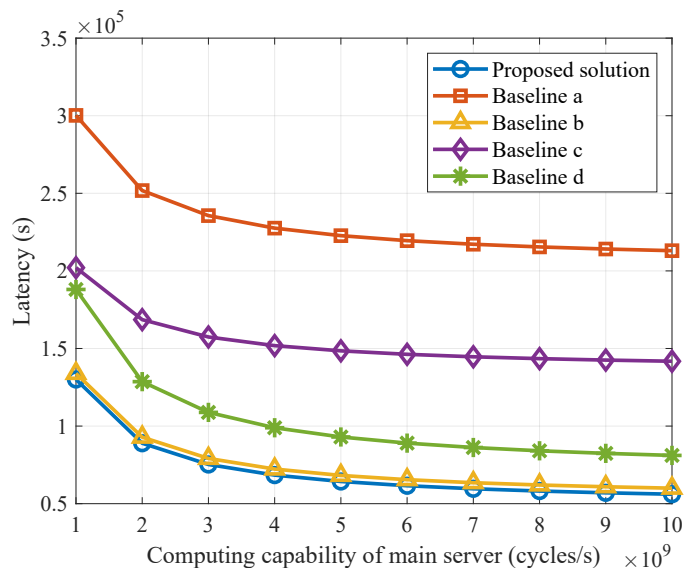


Fig. 7. The effect of LoRA rank on the number of steps required to reach the target loss value.

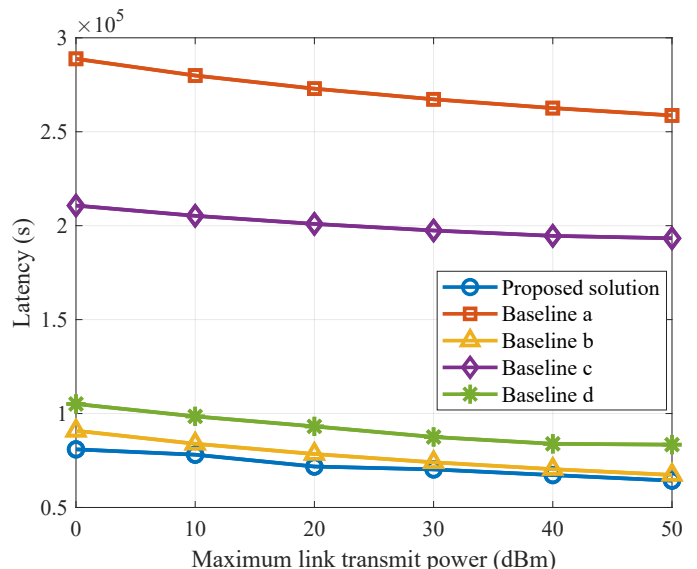


Fig. 8. The effect of LoRA rank on the number of steps required to reach the target loss value.

method.

VIII. CONCLUSION

In this paper, we propose a novel Federated Split Learning fine-tuned large language model framework (FedsLLM) designed for distributed training of large models on resource-constrained edge devices. FedsLLM reduces client computational workload by splitting the model, introducing federated servers for parallel training, and aggregating client models. The computational and communication costs are further reduced by LoRA, which significantly accelerates training by reducing latency. Considering the heterogeneity of client communication conditions and computational capability, and the substantial impact of rank on convergence speed and training

overhead, we propose a resource allocation and rank selection scheme. This scheme jointly optimizes subchannel allocation, power control, split location, and rank selection to enhance the training speed of FedsLLM over wireless networks. For the mixed-integer nonlinear programming delay minimization problem, we decompose it into four sub-problems based on different decision variables and propose solutions for each sub-problem. Subsequently, we present a Block Coordinate Descent (BCD)-based algorithm to solve this optimization problem. Simulation results demonstrate that FedsLLM achieves performance similar to centralized learning, and the proposed resource allocation and rank selection schemes significantly reduce training latency across different settings compared to traditional methods.

The findings in this paper highlight the potential of applying split federated learning to large model fine-tuning. Future research should focus on analyzing the effect of rank selection on convergence through theoretical derivations. Additionally, exploring an energy-efficient FedsLLM framework and extending it to different types of pre-trained models are promising directions for further investigation.

REFERENCES

- [1] K. Zhao, Z. Yang, C. Huang, X. Chen, and Z. Zhang, "Fedsllm: Federated split learning for large language models over communication networks," in *2024 International Conference on Ubiquitous Communication (Ucom)*. IEEE, 2024, pp. 438–443.
- [2] Z. Zhao, Z. Yang, Y. Hu, C. Zhu, M. Shikh-Bahaei, W. Xu, Z. Zhang, and K. Huang, "Compression ratio allocation for probabilistic semantic communication with RSMA," *IEEE Trans. Commun.*, pp. 1–1, 2025.
- [3] J. Achiam, S. Adler, S. Agarwal, L. Ahmad, I. Akkaya, F. L. Aleman, D. Almeida, J. Altenschmidt, S. Altman, S. Anadkat *et al.*, "Gpt-4 technical report," *arXiv preprint arXiv:2303.08774*, 2023.
- [4] A. Chowdhery, S. Narang, J. Devlin, M. Bosma, G. Mishra, A. Roberts, P. Barham, H. W. Chung, C. Sutton, S. Gehrmann *et al.*, "Palm: Scaling language modeling with pathways," *Journal of Machine Learning Research*, vol. 24, no. 240, pp. 1–113, 2023.
- [5] J. Kaplan, S. McCandlish, T. Henighan, T. B. Brown, B. Chess, R. Child, S. Gray, A. Radford, J. Wu, and D. Amodei, "Scaling laws for neural language models," *arXiv preprint arXiv:2001.08361*, 2020.
- [6] A. J. Thirunavukarasu, D. S. J. Ting, K. Elangovan, L. Gutierrez, T. F. Tan, and D. S. W. Ting, "Large language models in medicine," *Nature medicine*, vol. 29, no. 8, pp. 1930–1940, 2023.
- [7] S. Wu, O. Irsoy, S. Lu, V. Dabravolski, M. Dredze, S. Gehrmann, P. Kambadur, D. Rosenberg, and G. Mann, "Bloomberggpt: A large language model for finance," *arXiv preprint arXiv:2303.17564*, 2023.
- [8] T. Fan, Y. Kang, G. Ma, W. Chen, W. Wei, L. Fan, and Q. Yang, "Fate-llm: A industrial grade federated learning framework for large language models," *arXiv preprint arXiv:2310.10049*, 2023.
- [9] W. Kuang, B. Qian, Z. Li, D. Chen, D. Gao, X. Pan, Y. Xie, Y. Li, B. Ding, and J. Zhou, "Federatedscope-llm: A comprehensive package for fine-tuning large language models in federated learning," in *Proceedings of the 30th ACM SIGKDD Conference on Knowledge Discovery and Data Mining*, 2024, pp. 5260–5271.
- [10] R. Ye, W. Wang, J. Chai, D. Li, Z. Li, Y. Xu, Y. Du, Y. Wang, and S. Chen, "Openfedllm: Training large language models on decentralized private data via federated learning," in *Proceedings of the 30th ACM SIGKDD conference on knowledge discovery and data mining*, 2024, pp. 6137–6147.
- [11] J. Konečný, H. B. McMahan, F. X. Yu, P. Richtárik, A. T. Suresh, and D. Bacon, "Federated learning: Strategies for improving communication efficiency," *arXiv preprint arXiv:1610.05492*, 2016.
- [12] P. Vepakomma, O. Gupta, T. Swedish, and R. Raskar, "Split learning for health: Distributed deep learning without sharing raw patient data," *arXiv preprint arXiv:1812.00564*, 2018.
- [13] Z. Lin, G. Zhu, Y. Deng, X. Chen, Y. Gao, K. Huang, and Y. Fang, "Efficient parallel split learning over resource-constrained wireless edge networks," *IEEE Transactions on Mobile Computing*, vol. 23, no. 10, pp. 9224–9239, 2024.
- [14] Z. Lin, G. Qu, X. Chen, and K. Huang, "Split learning in 6g edge networks," *IEEE Wireless Communications*, 2024.
- [15] C. Thapa, P. C. M. Arachchige, S. Camtepe, and L. Sun, "Splitfed: When federated learning meets split learning," in *Proceedings of the AAAI conference on artificial intelligence*, vol. 36, no. 8, 2022, pp. 8485–8493.
- [16] E. J. Hu, Y. Shen, P. Wallis, Z. Allen-Zhu, Y. Li, S. Wang, L. Wang, W. Chen *et al.*, "Lora: Low-rank adaptation of large language models," *ICLR*, vol. 1, no. 2, p. 3, 2022.
- [17] Y. Sheng, S. Cao, D. Li, C. Hooper, N. Lee, S. Yang, C. Chou, B. Zhu, L. Zheng, K. Keutzer *et al.*, "S-lora: Serving thousands of concurrent lora adapters," *arXiv preprint arXiv:2311.03285*, 2023.
- [18] A. Radford, J. Wu, R. Child, D. Luan, D. Amodei, I. Sutskever *et al.*, "Language models are unsupervised multitask learners," *OpenAI blog*, vol. 1, no. 8, p. 9, 2019.
- [19] J. Novikova, O. Dušek, and V. Rieser, "The e2e dataset: New challenges for end-to-end generation," *arXiv preprint arXiv:1706.09254*, 2017.
- [20] P. Joshi, C. Thapa, S. Camtepe, M. Hasanuzzamana, T. Scully, and H. Afl, "Splitfed learning without client-side synchronization: Analyzing client-side split network portion size to overall performance," *arXiv preprint arXiv:2109.09246*, 2021.
- [21] Z. Lin, X. Hu, Y. Zhang, Z. Chen, Z. Fang, X. Chen, A. Li, P. Vepakomma, and Y. Gao, "Splitlora: A split parameter-efficient fine-tuning framework for large language models," *arXiv preprint arXiv:2407.00952*, 2024.
- [22] M. Chen, D. Gündüz, K. Huang, W. Saad, M. Bennis, A. V. Feljan, and H. V. Poor, "Distributed learning in wireless networks: Recent progress and future challenges," *IEEE Journal on Selected Areas in Communications*, vol. 39, no. 12, pp. 3579–3605, 2021.
- [23] K. Lee, M. Lam, R. Pedarsani, D. Papailiopoulos, and K. Ramchandran, "Speeding up distributed machine learning using codes," *IEEE Transactions on Information Theory*, vol. 64, no. 3, pp. 1514–1529, 2017.
- [24] D. Shi, L. Li, R. Chen, P. Prakash, M. Pan, and Y. Fang, "Toward energy-efficient federated learning over 5g+ mobile devices," *IEEE Wireless Communications*, vol. 29, no. 5, pp. 44–51, 2022.
- [25] J. Xu and H. Wang, "Client selection and bandwidth allocation in wireless federated learning networks: A long-term perspective," *IEEE Transactions on Wireless Communications*, vol. 20, no. 2, pp. 1188–1200, 2020.
- [26] Y. Jiao, P. Wang, D. Niyato, B. Lin, and D. I. Kim, "Toward an automated auction framework for wireless federated learning services market," *IEEE Transactions on Mobile Computing*, vol. 20, no. 10, pp. 3034–3048, 2020.
- [27] X. Chen, G. Zhu, Y. Deng, and Y. Fang, "Federated learning over multi-hop wireless networks with in-network aggregation," *IEEE Transactions on Wireless Communications*, vol. 21, no. 6, pp. 4622–4634, 2022.
- [28] R. Chen, D. Shi, X. Qin, D. Liu, M. Pan, and S. Cui, "Service delay minimization for federated learning over mobile devices," *IEEE Journal on Selected Areas in Communications*, vol. 41, no. 4, pp. 990–1006, 2023.
- [29] W. Wu, M. Li, K. Qu, C. Zhou, X. Shen, W. Zhuang, X. Li, and W. Shi, "Split learning over wireless networks: Parallel design and resource management," *IEEE Journal on Selected Areas in Communications*, vol. 41, no. 4, pp. 1051–1066, 2023.
- [30] Z. Lin, G. Qu, W. Wei, X. Chen, and K. K. Leung, "Adaptsfl: Adaptive split federated learning in resource-constrained edge networks," *arXiv preprint arXiv:2403.13101*, 2024.
- [31] X. Liu, Y. Deng, and T. Mahmoodi, "Wireless distributed learning: A new hybrid split and federated learning approach," *IEEE Transactions on Wireless Communications*, vol. 22, no. 4, pp. 2650–2665, 2022.
- [32] L. U. Khan, M. Guizani, A. Al-Fuqaha, C. S. Hong, D. Niyato, and Z. Han, "A joint communication and learning framework for hierarchical split federated learning," *IEEE Internet of Things Journal*, vol. 11, no. 1, pp. 268–282, 2023.
- [33] J. Shen, N. Cheng, X. Wang, F. Lyu, W. Xu, Z. Liu, K. Aldubaikhy, and X. Shen, "Ringsfl: An adaptive split federated learning towards taming client heterogeneity," *IEEE Transactions on Mobile Computing*, vol. 23, no. 5, pp. 5462–5478, 2023.
- [34] K. He, X. Zhang, S. Ren, and J. Sun, "Deep residual learning for image recognition," in *Proceedings of the IEEE conference on computer vision and pattern recognition*, 2016, pp. 770–778.
- [35] K. Simonyan and A. Zisserman, "Very deep convolutional networks for large-scale image recognition," *arXiv preprint arXiv:1409.1556*, 2014.
- [36] A. Krizhevsky, I. Sutskever, and G. E. Hinton, "Imagenet classification with deep convolutional neural networks," *Advances in neural information processing systems*, vol. 25, 2012.

- [37] J. Jiang, H. Jiang, Y. Ma, X. Liu, and C. Fan, "Low-parameter federated learning with large language models," in *International Conference on Web Information Systems and Applications*. Springer, 2024, pp. 319–330.
- [38] T. Fan, Y. Kang, G. Ma, L. Fan, K. Chen, and Q. Yang, "Fedcollm: A parameter-efficient federated co-tuning framework for large and small language models," *arXiv preprint arXiv:2411.11707*, 2024.
- [39] C. Xu, J. Li, Y. Liu, Y. Ling, and M. Wen, "Accelerating split federated learning over wireless communication networks," *IEEE Transactions on Wireless Communications*, vol. 23, no. 6, pp. 5587–5599, 2023.
- [40] G. Zhu, Y. Deng, X. Chen, H. Zhang, Y. Fang, and T. F. Wong, "Esfl: Efficient split federated learning over resource-constrained heterogeneous wireless devices," *IEEE Internet of Things Journal*, 2024.
- [41] X. Hu, L. Wang, K.-K. Wong, M. Tao, Y. Zhang, and Z. Zheng, "Edge and central cloud computing: A perfect pairing for high energy efficiency and low-latency," *IEEE Transactions on Wireless Communications*, vol. 19, no. 2, pp. 1070–1083, 2019.